The comparison with IV-18 does not show as pronounced an effect.

The effects of the solvent are complex and difficult to interpret. Solvent effects on the rate enhancements in Table III are conformational in origin, since in each solvent the chemical reactions of I, II, III, and IV are the same: This means that the probability of a CH_2 group being in the reactive volume adjacent to the ketone oxygen of the chromophore is sensitive to solvent. Many factors can affect this probability. Among them are the interaction of the ester dipoles with the solvent dipoles and favorable interactions in poor solvents between CH_2 groups of the chain with the aromatic rings of the benzophenone. Intramolecular interactions between CH_2 groups in the chain are unlikely to play an important role because, for chains as short as 17 carbons, the pentane effect makes nonbonded interactions between remote CH_2 groups extremely improbable.

Solvent effects on product distribution are even more difficult to interpret because a major component of that effect could be solvent influences on the partitioning of the biradical **2** to starting ketone and to product.

Conclusion

Molecules I, II, and III possess flexible chains containing substituents which perturb the population of rotational states corresponding to the C(1)–C(2) and C(3)–C(4) bonds of the alkyl chain in IV. In addition, the substituents make small changes in bond and rotational angles. Rotational isomeric state model calculations suggest that the former effects should increase the cyclization probability and hence the rate constant for intramolecular reaction. Flash photolysis measurements indicate that I, II, and III undergo intramolecular reactions respectively 2.5, 6, and 9 times more readily than the molecule IV with the same length alkyl chain.

Acknowledgment. U.M. and M.A.W. would like to thank the National Engineering and Science Research Council of Canada for its financial assistance. B.D. and H.J.S. would like to thank the Minister für Wissenschaft und Forschung des Landes Nordrhein-Westfalen, Germany, and the Fonds der chemischen Industrie.

References and Notes

(1) (a) P. J. Flory, "Statistical Mechanics of Chain Molecules", Wiley, New York, 1969; (b) A. J. Hopfinger "Conformational Properties of Macromolecules", Academic Press, New York, 1973; (c) H. Yamakawa "Modern Theory of Polymer Solutions", Harper and Row, New York, 1971.
(2) B. Dors, F. Kamper, and H. J. Schafer, 2nd International Symposium on Organic Free Radicals, July 17–23, 1977, Aix-en Provence, France, Extended Abstracts, p 515, Colloques Internationaux du CNRS.
(3) (a) W. Kuhn, *Kolloid-Z.*, **68**, 2 (1934); (b) H. Morawetz, *Pure Appl. Chem.*, **38**, 267 (1974); (c) H. Morawetz and N. Goodman, *J. Polym. Sci., Part C*, **31**, 177 (1970); (d) N. Goodman and H. Morawetz, *J. Polym. Sci., Part A-2*, **9**, 1657 (1971); (e) H. Morawetz and N. Goodman, *Macromolecules*, **3**, 699 (1970); (f) M. Sisido, *ibid.*, **4** 737 (1971); (g) M. Sisido, H. Takagi, Y. Imanishi, and T. Higashimura, *ibid.*, **10**, 125 (1977); (h) H. Takaji, M. Sisido, Y. Imanishi, and T. Higashimura, *Bull. Chem. Soc. Jpn.*, **50**, 1807 (1977); (i) M. Sisido and K. Shimada, *J. Am. Chem. Soc.*, **99**, 7785 (1977).
(4) (a) G. Wilemski and M. Fixman, *J. Chem. Phys.*, **60**, 866 878 (1974); (b) M. Fixman, *ibid.*, **69**, 1527, 1538 (1978).
(5) M. A. Winnik, *Acc. Chem. Res.*, **10**, 173 (1977).
(6) (a) M. A. Winnik, S. Basu, C. K. Lee, and D. S. Saunders, *J. Am. Chem. Soc.*, **98**, 2928 (1976); (b) M. A. Winnik, A. Lemire, D. S. Saunders, and C. K. Lee, *ibid.*, **98**, 2000 (1976); (c) M. A. Winnik and A. Lemire, *Chem. Phys. Lett.*, **46**, 283 (1977).
(7) (a) R. Breslow, J. Rothbard, F. Herman, and M. L. Rodriquez, *J. Am. Chem. Soc.*, **100**, 1213 (1978); (b) R. Breslow, *Chem. Soc. Rev.*, **1**, 553 (1972).
(8) (a) R. E. Trueman and S. G. Whittington, *J. Phys. A: Gen. Phys.*, **5**, 1664 (1972). (b) In the language of graph theory, a tadpole is a graph with a single intersection involving only one terminus of the graph or walk.
(9) D. S. Saunders and M. A. Winnik, *Macromolecules*, **11**, 18, 25 (1978). Note that in the second paper (pp 31, 32 and Tables IV and V), discussion referring to the configuration about the C(2)–C(3) bond in fact refers to the rotational state of the C(1)–C(2) bond.
(10) D. Schuster and T. Weil, *Mol. Photochem.*, **6**, 477 (1972).
(11) M. A. Winnik and U. Maharaj, *Macromolecules*, previous paper in this issue.
(12) Reference 1a, p 213.

A Determination of Polymer Number-Averaged and Weight-Averaged Molecular Weight Using Photon Correlation Spectroscopy

J. C. Selser

IBM Research Laboratory, San Jose, California 95193. *Received April 20, 1979*

ABSTRACT: A method is developed whereby the autocorrelation spectra of light scattered inelastically from dilute polymer solutions can be used to determine polymer number-averaged and weight-averaged molecular weights. The method is based on transforming the polymer z-averaged diffusion coefficient and its relative dispersion, extracted from a cumulants analysis of the spectra, into number-averaged and weight-averaged molecular weights. To do this, experimentally determined constants from diffusion coefficient versus molecular weight studies are employed. The range of validity in the resulting transform expressions is subject to certain restrictions in the width and in the magnitudes of higher moments of the polymer molecular weight distribution. The expressions derived have particular potential usefulness in the determination of $\bar{M}_n$ and $\bar{M}_w$ for rodlike polymers. $\bar{M}_n$ and $\bar{M}_w$ values determined using these expressions to analyze narrow and intermediate molecular weight polystyrene samples are in good agreement with both the manufacturers data and gel permeation chromatographic analyses.

The characterization of polymer molecular weight distributions using time-average or so-called "elastic" light-scattering techniques continues to merit investigation.[1,2] During the past decade, though, inelastic (or quasielastic) light-scattering techniques have also been successfully applied to this endeavor.[3] In inelastic scattering, an analysis is made of phase fluctuations in the scattered light using either the power spectral density or

0024-9297/79/2212-0909$01.00/0

the autocorrelation spectrum (ACS) of light scattered quasielastically from a dilute, polydisperse system of independently diffusing polymer molecules in an effectively "invisible" solvent. Digital photopulse processing electronics in conjunction with digital correlators have made photon correlation spectroscopy (PCS) the most efficient method of using quasielastically scattered light to study polymer solutions. When the polymer molecules scatter light as Rayleigh particles, temporal behavior in the scattered light may be related to sample diffusive processes via the field autocorrelation function $|G^{(1)}(\tau)|$:[3,4]

$$|G^{(1)}(\tau)| = \int_0^\infty f(\Gamma)e^{-\Gamma\tau}\,d\Gamma \tag{1}$$

where $f(\Gamma)$ is the distribution function of the relaxation parameter, $\Gamma \equiv DK^2$. D is the polymer center-of-mass diffusion coefficient and the magnitude of the scattering vector $K = (4\pi n/\lambda_0)\sin\theta/2$ with n the solvent index of refraction, θ the scattering angle, and λ_0 the vacuum wavelength of the incident light. A distribution in the molecular weight of the polymer scatterers, $h(M)$, gives rise to the relaxation parameter distribution function, $f(\Gamma)$. Three methods of analyzing $|G^{(1)}|$ to extract information concerning $h(M)$ are currently employed. In the first, a parameterized form of $h(M)$ is assumed, and the parameters of interest, $\bar{M}_n$ for example, are extracted from the ACS.[3] In the second, $h(M)$ is estimated by numerical inversion of the ACS.[5] In the third, $\exp(-\Gamma\tau)$ is expanded in a Taylor series about $\bar{\Gamma}$ inside the integral in expression 1 and the integration performed.[4] A fit to the resulting expression yields coefficients that are then translated into parameters of interest. The first approach has the disadvantage of requiring a-priori knowledge of $h(M)$ to yield valid results. The second is complicated, requires relatively sophisticated computing capability, and places a large burden on the statistical quality of the ACS in order to ensure reliable results.[4,9] By contrast, the method of cumulants requires no special assumptions about the form of $h(M)$, requires only modest computational capability, and is easy to implement. For these reasons, it was decided to investigate, theoretically and experimentally, the characterization of polymer molecular weight distributions by applying the cumulant method of analyzing the ACS of light scattered quasielastically from dilute polymer systems. Although the method of cumulants has been used before in analyzing inelastic light-scattering results to assess polymer molecular weight,[6] the study presented here is more general and thorough in its treatment of the problem and uncovers interesting and significant results that have not been presented elsewhere.

Theory

When all the polymer molecules in solution have the same polarizability, $|G^{(1)}(\tau)|$ may be written:[4]

$$|G^{(1)}(\tau)| = \int_0^\infty f(\Gamma)e^{-\Gamma\tau}\,d\Gamma \tag{1a}$$

with

$$f(\Gamma) = \sum_i \langle I\rangle_i \delta(\Gamma - \Gamma_i) \tag{2}$$

where $\langle I\rangle_i$ and Γ_i are the average intensity and decay parameter, respectively, for particles of the ith molecular weight and $\delta(\,)$ is the Dirac delta distribution. It follows that

$$|G^{(1)}(0)| = \int_0^\infty f(\Gamma)\,d\Gamma = \sum_i \langle I\rangle_i = \langle I\rangle \tag{3}$$

the total time-averaged intensity of light scattered by all polymer molecules in the scattering volume. Expanding $\exp(-\Gamma\tau)$ about an average in the relaxation parameter, $\bar{\Gamma}$, $|G^{(1)}(\tau)|$ can be expressed as[4]

$$|G^{(1)}(\tau)| = e^{-\bar{\Gamma}\tau}\left\{1 + \frac{\mu_2}{2!}\tau^2 + \frac{\mu_3}{3!}\tau^3 + \ldots\right\} \tag{4}$$

with

$$\mu_n = \langle(\Gamma - \bar{\Gamma})^n\rangle \tag{5}$$

so that μ_2, for example, is the mean-squared deviation in Γ about $\bar{\Gamma}$. By direct substitution,[4]

$$\bar{\Gamma} = \bar{D}K^2 \tag{6}$$

and

$$\langle D\rangle_z \equiv \bar{D} = \frac{\sum_i \langle I\rangle_i D_i}{\sum_i \langle I\rangle_i} = \frac{\sum_i N_i m_i^2 D_i}{\sum_i N_i m_i^2} \tag{7}$$

where m_i and D_i are the mass and diffusion coefficient, respectively, of polymer molecules of the ith molecular weight.

It is seen that the averaged quantities extracted from autocorrelation spectra using the method of cumulants are mass-squared weighted or "z"-averaged quantities. Generally, moments beyond μ_2 are experimentally extremely difficult to determine, as they are "buried" in statistical uncertainties in the ACS. In addition, it is useful to rewrite expression 4 in the form:

$$|G^{(1)}(\tau)| = e^{-\tau/\tau_c}\left\{1 + \frac{\delta_z}{2}(\tau/\tau_c)^2\right\} \tag{8}$$

with the characteristic time of the spectral relaxation

$$\tau_c = 1/\langle D\rangle_z K^2 \tag{9}$$

and the relative dispersion in the diffusion coefficient about its z average,

$$\delta_z = \frac{\mu_2}{\bar{\Gamma}^2} = \frac{\langle(D - \langle D\rangle_z)^2\rangle}{\langle D\rangle_z^2} \tag{10}$$

The results presented in this paper are based on unclipped autocorrelation spectra from self-beat experiments. These spectra may be represented by an expression of the form:[4]

$$G^{(2)}(\tau) = A|G^{(1)}(\tau)|^2 + B \tag{11}$$

where A is a proportionality constant incorporating the effect on the spectrum of partial coherence in the scattered light and B is the spectral base line.

As will be shown in the Discussion section, it is a straightforward matter to extract $\langle D\rangle_z$ and δ_z from autocorrelation spectra that are of the form of (11). Calculating molecular weights from these two parameters requires knowledge of the relationship between polymer diffusion coefficient and molecular weight as well. This power law relationship, valid over an experimentally

$$D = CM^{-\nu} \tag{12}$$

determined molecular weight range, is well-known, semiempirical in nature, and based on hydrodynamic considerations. The constants C and ν are determined experimentally, and values of ν for both biopolymers and synthetic polymers fall in the range $^1/_3 \lesssim \nu \lesssim 1$ with the lower and upper limits for spheres and rods, respectively, and intermediate values for coils, disks, etc. Although this relationship has been employed in the interpretation of

inelastic light-scattering data in various ways before,[3,5,6] the approach used to employ it and the results developed here are unique.

To transform $\langle D\rangle_z$ and δ_z into parameters relating to the polymer number-averaged molecular weight, expression 12 is substituted for D in eq 7 and 10, taking advantage of the proportion between polymer mass and molecular weight. The resulting expressions are converted to number-averaged quantities through multiplication by unity in the form $\sum_i N_i/\sum_i N_i$. The expressions inside the (number) averaging brackets are then expanded in a Taylor series about the number-averaged molecular weight and formal averaging is carried out. The resulting equations have only z-averaged quantities on the left-hand side and only number-averaged quantities and their moments on the right-hand side. It is worth noting that no explicit molecular weight distribution function is used. It is also worth noting that this method can be used to transform $\langle D\rangle_z$ and δ_z into other types of useful and meaningful number averages and their moments. For example, $\langle D\rangle_z$ and δ_z from inelastic light-scattering measurements on membrane vesicle suspensions were converted to vesicle number-averaged radii and their relative dispersions using a different version of this approach.[7,8] To illustrate the procedure, the conversion of $\langle D\rangle_z$ is carried out explicitly:

$$\langle D\rangle_z = \frac{\sum_i N_i m_i^2 D_i}{\sum_i N_i m_i^2} = \frac{\sum_i N_i M_i^2 (C M_i^{-\nu})}{\sum_i N_i M_i^2} \frac{\sum_i N_i}{\sum_i N_i} \quad (13)$$

$$\langle D\rangle_z = C\langle M^{2-\nu}\rangle_n / \langle M^2\rangle_n \quad (14)$$

where the n subscripting of the brackets denotes number averaging. After expansion and averaging,

$$\langle D\rangle_z = C\langle M\rangle_n^{-\nu}\{1 + [(2-\nu)(1-\nu)/2]\delta_{2n} - [\nu(2-\nu)(1-\nu)/6]\delta_{3n} + \ldots\}/(1+\delta_{2n}) \quad (15)$$

where δ_{2n}, δ_{3n}, etc., are the normalized second, third, etc., moments of the molecular weight distribution. Specifically:

$$\delta_{2n} = \langle (M - \langle M\rangle_n)^2\rangle_n / \langle M\rangle_n^2 \quad (16)$$

and

$$\delta_{3n} = \langle (M - \langle M\rangle_n)^3\rangle_n / \langle M\rangle_n^3 \quad (17)$$

As it stands, expression 15 is reasonable. It says, for example, that as the width of the molecular weight distribution increases, $\langle D\rangle_z$ decreases because higher molecular weight species contribute more to it than do lower molecular weight species. On the other hand, the skewness of the distribution could increase so as to favor lower molecular weight species, and the term containing δ_{3n} might then outweigh the influence of the width term—note the sign difference—resulting in an increase in $\langle D\rangle_z$. The conversion of δ_z is carried out in the same way, with

$$\delta_z + 1 = \frac{\langle M^2\rangle_n \langle M^{2-2\nu}\rangle_n}{\langle M^{2-\nu}\rangle_n^2} = (1+\delta_{2n})\{1 + (1-\nu)\times(1-2\nu)\delta_{2n} - [2\nu(1-2\nu)(1-\nu)/3]\delta_{3n} + \ldots\}/\{1 + [(1-\nu)(2-\nu)/2]\delta_{2n} - [\nu(2-\nu)(1-\nu)/6]\delta_{3n} + \ldots\}^2 \quad (18)$$

where for convenience in computation $\delta_z + 1$ is used instead of δ_z. Because only $\langle D\rangle_z$ and δ_z can be reliably extracted from the ACS, eq 15 and 18 must be truncated after terms containing δ_{2n}. This restriction amounts to assuming that the combined influence of the third and higher moments in these expressions is negligible. One of the tasks of this study is to examine experimentally the consequences of truncating these expressions after their second moments. The truncated versions are:

$$\langle D\rangle_z = C\langle M\rangle_n^{-\nu} \frac{1 + [(2-\nu)(1-\nu)/2]\delta_{2n}}{1+\delta_{2n}} \quad (19)$$

$$\delta_z = \frac{\nu^2}{4} \frac{\delta_{2n}[4 + (1-\nu)(\nu-5)\delta_{2n}]}{[1 + [(2-\nu)(1-\nu)/2]\delta_{2n}]^2} \quad (20)$$

As will be demonstrated later, a variety of worthwhile and interesting systems may be successfully analyzed using eq 19 and 20.

Knowing C and ν, the usual procedure is to measure $\langle D\rangle_z$ and δ_z, and from eq 20, δ_{2n} is calculated and substituted into eq 19, and $\langle M\rangle_n$ is then computed. Since

$$\bar{M}_w = \sum_i N_i M_i^2 / \sum_i N_i M_i = \langle M^2\rangle_n / \langle M\rangle_n = \langle M\rangle_n (1+\delta_{2n})$$

$$\delta_{2n} = \bar{M}_w/\bar{M}_n - 1 \quad (21)$$

Thus from δ_{2n}, $\bar{M}_w/\bar{M}_n$ is known, and in conjunction with $\langle M\rangle_n$, $\langle M\rangle_w$ is calculated. The relative dispersion in the molecular weight, δ_{2n}, also appears in the light-scattering literature denoted as "U", referring to the German word for dispersivity, "uneinheitlichkeit".

More careful consideration of expressions 19 and 20 reveals several noteworthy features. As $\delta_{2n} \to 0$ or as $\nu \to 1$, that is for narrow distributions or for rodlike polymers, these expressions have particularly simple forms: As $\delta_{2n} \to 0$

$$\langle D\rangle_z = C\langle M\rangle_n^{-\nu} \quad (22)$$

$$\delta_z = \nu^2 \delta_{2n} \quad (23)$$

While for reasonable δ_{2n}, as $\nu \to 1$

$$\langle D\rangle_z = C/\bar{M}_w \quad (24)$$

and

$$\delta_z = \nu^2 \delta_{2n} \quad (23a)$$

as before. As δ_{2n} grows, $\langle D\rangle_z$ in eq 19 tends to zero, as at first glance it seems it should but for larger values of δ_{2n} (≈ 1 so $\bar{M}_w/\bar{M}_n \approx 2$), and at values of ν not close to 1, δ_z begins to behave nonphysically. This strange behavior in δ_z is illustrated by the dashed portion of the curves in Figure 1. This nonphysical behavior stems from the constraint that the distribution remain very symmetric regardless of the magnitude of δ_{2n}. The consequences of this assumption are presented using a hypothetical ($\nu < 1$), normalized, rectangular distribution for illustrative purposes, in Figure 2. While the width of a real distribution may move to indefinitely larger molecular weight, it is constrained to have some positive, minimum value (M_{min}) in its molecular weight distribution. This means that a real distribution cannot grow indefinitely wide in both directions without becoming skewed. The truncated, symmetric distribution, by contrast, is free to extend its width indefinitely in both the higher and lower molecular weight directions. Consequently, nonphysically small positive and even negative molecular weight values may be included in the distribution. Eventually, δ_z begins to decrease with increasing δ_{2n}, which is not physically possible, and even becomes negative once the width of the distribution is sufficiently great. To avoid using expressions 19 and 20 where they are no longer valid, it is required that only the portion of the δ_z vs. δ_{2n} curve having a positive slope, i.e, $\partial\delta_z/\partial\delta_{2n} > 0$, be used. The basis for this criterion is the intuitive requirement that for a real,

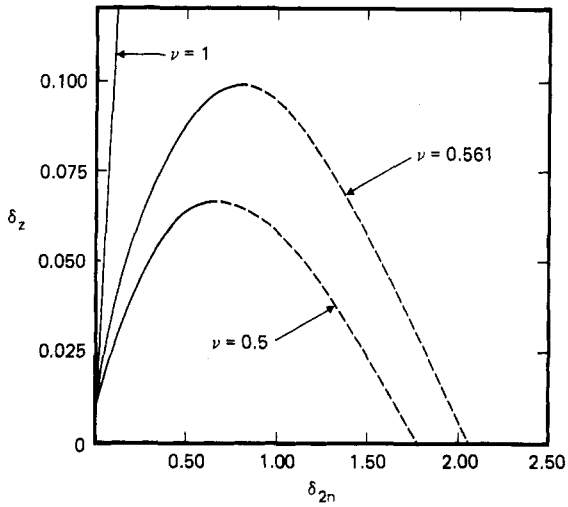

Figure 1. Plot of δ_z as a function of δ_{2n} for several values of ν. The dashed portions of the curves indicate the regions of nonphysical behavior referred to in the text. Note the scale difference between the axes and that for $\nu = 1$; there is no nonphysical region.

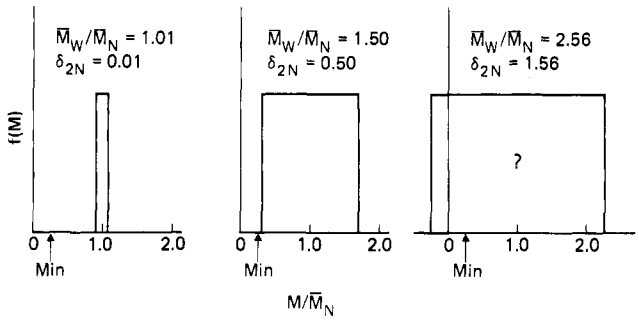

Figure 2. Picture of how a hypothetical symmetric distribution becomes nonphysical as its width increases thereby giving rise to the dashed portions of Figure 1. Note that distribution widths are not to scale.

essentially symmetric distribution, δ_z increase monotonically with increasing δ_{2n}. By calculating the slope of the δ_z vs. δ_{2n} curve using eq 2 and requiring the result to be positive, the following condition on the ν, δ_{2n} combination is found:

$$(1 - \nu)(7 - 2\nu)\delta_{2n} < 2 \qquad (25)$$

It is important to recognize that for more rodlike polymers for which $\nu \rightarrow 1$, the dependence of $\langle D \rangle_z$ and δ_z on the moments of the molecular weight distribution becomes progressively weaker, eq 19 and 20 go over into the simpler eq 24 and 23, and the condition 25 will tolerate practically any value of δ_{2n}. This behavior is graphically demonstrated for $\nu = 1$ in Figure 1. This result is important as it shows that application of the method of cumulants to the analysis of autocorrelation spectra for the purpose of determining polymer molecular weights is particularly suited to rodlike polymers. It must be pointed out here, however, that there is another condition imposed on δ_z, and therefore indirectly on δ_{2n}, when using the method of cumulants. The origin and consequences of this additional condition will be discussed further in the Data Analysis section.

Finally, from eq 23 it is seen that the effect of the width of the distribution is reduced by a factor which depends on the square of ν. While this dependence results in a lower limit in the detectability of the polydispersity, δ_{2n} (see Discussion of Results section), it also allows reasonably broad distributions to be measured using the methods developed here.

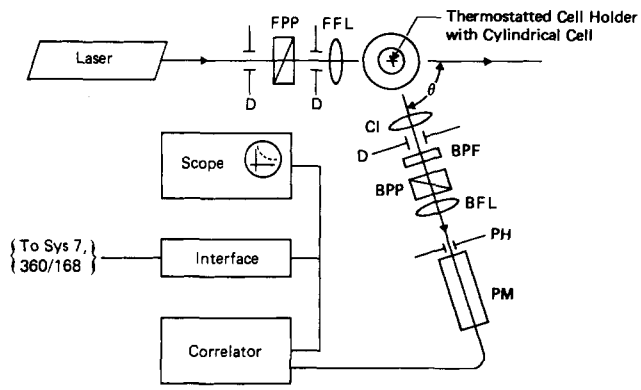

Figure 3. Schematic diagram of the PCS spectrometer. The designations of the components are explained in the text.

Experimental Section

Apparatus. The apparatus used in making the measurements reported here is an in-house variable-angle laser-light-scattering photometer mounted on a commercial vibrationally isolated air suspension table (Newport Research Corp., Fountain Valley, Calif.). The photopulse output of the photometer is connected to a digital correlator (Langley-Ford Instruments, Amherst, Mass.). The sample cell is a precision bore (5 mm i.d., 7 mm o.d.) fused silica tube sealed and aligned vertically in a cell holder by machined black Teflon stoppers at its top and bottom. The sample volume is about 3/4 mL. Two valved stainless steel needles allow sample entry into and exit from the cell. A larger (40 mm o.d., 1 cm high) fused silica window is held concentrically to the sample cell by seating and sealing it between two machined aluminum pieces that also serve to align the cell by seating the Teflon stoppers. The space between the cell and the window is filled with spectroscopic grade glycerol, whose refractive index is very close to that of fused silica. This index matching helps reduce spurious scattering at the sample cell walls and helps reduce diffraction in the incident laser beam. The glycerol also provides thermal stability at the sample. The sample cell assembly is insulated by a thick glass–epoxy housing, and sample temperature is controlled by heating or cooling the aluminum pieces, which are jacketed for that purpose, by circulating a temperature-controlled fluid through the jackets. A calibrated thermistor-probe immersed in the glycerol can be used to measure the sample temperature.

The sample is excited by the 6471 Å wavelength line of a Krypton ion laser (Model 165, Spectra Physics, Mountain View, Calif.). A Glan-laser polarizing prism (FPP) (see Figure 3) ensures the vertical polarization of light incident on the sample while two diaphrams (D) are used to block the passage of any stray reflections through the sample. The front focusing lens (FFL) has a long focal length (14 cm) and gently focuses the incident light to a spot about 80 μm in diameter in the sample.

The scattering angle is read directly from the optical display of the rotary table. The angular accuracy of the rotary table is better than 1 min of arc. Scattered light is collected by a lens at its focal length in the far field (CL) and sent through a diaphram (D) whose opening is set to about one spatial coherence area. The accepted light then passes through a narrow bandpass filter (BPF) centered at the laser wavelength and passes through a Glan-Taylor polarizing prism (PP) whose pass axis is set parallel to the polarization direction of the incident laser beam. The remaining light is then focused (BFL) onto a 50 μm pinhole (PH). From the pinhole, the light fans out onto the phototube photocathode (Model 9558A, EMI Gencom, Plainview, N.Y.). A microscope is used to examine the scattering volume before the photomultiplier is set in place. This is possible because the post-sample optics image the scattering volume at the plane of the pinhole. This visual examination of the scattering volume to check vertical alignment and to ensure that the sample is "OK" is critical. The phototube is socketed in a shielded housing with an integral amplifier-discriminator at its base (Model 1102, Products for Research, Danvers, Mass.). The phototube housing also contains two defocusing magnets at its front end, and as a result, the room-temperature (21–22 °C) dark count of the tube is only about

250–300 Hz. A very stable high-voltage power supply (HVS-1, Princeton Applied Research, Princeton, N.J.) maintains the photocathode voltage at −1400 V, which is determined to be optimally stable and in the linear voltage regime for this tube.

The output pulses of the amplifier–discriminator are sent to the autocorrelator where the photopulse correlation spectrum is computed. The evolving ACS is monitored on a display oscilliscope (Model 1220A, Hewlett-Packard Co., Palo Alto, Calif.), and when each spectrum is deemed satisfactory, it is transferred to an IBM System-7 processing computer for temporary storage. After the requisite number of runs (spectra) necessary to complete an experiment have been made, these runs are sent to an IBM-360/168 for analysis. Spectra can also be permanently stored for future reference.

Sample Preparation. Four polystyrene standards and one blend of three of these standards were prepared for measurement. Two of the standards were obtained from the National Bureau of Standards (NBS), Washington, D.C. These two were the narrow molecular weight distribution standard 705 and the broad molecular weight distribution standard 706. The other two were narrow distribution standards obtained from the Pressure Chemical Company (PC) of Pittsburgh, Pa. All samples were dissolved in distilled-in-glass 2-butanone (Burdick and Jackson Labs, Muskegon, Mich.) by being shaken overnight on a wrist shaker. Sample flasks were acid cleaned and rinsed with filtered butanone before samples were prepared in them. Prior to use, sample cells were acid cleaned, rinsed with THF, acetone, and methanol, and then placed for several hours in a 2-propanol refluxing cell cleaner. Samples were then filtered into the sample cell. Each dilution of each sample was filtered through its own set of two fluoropore 0.2-μm filters (Millipore Corp., Bedford, Mass.). These filters were placed back-to-back in the filter holder. All measurements were made at room temperature (21–22 °C). Since the lab has its own air conditioner and temperature control is excellent, the room temperature was essentially constant during each experiment. Use of the circulating temperature controller was not necessary. The sample temperature was taken to be the room temperature after 20–30 min. A laboratory thermometer was used to measure temperature, and reading the thermometer resulted in a temperature measurement uncertainty of about 0.2 °C.

Data Analysis. As mentioned earlier, analysis of autocorrelation spectra using the method of cumulants can be made particularly simple. To do this, expression 8 for $|G^{(1)}(\tau)|$ is first modified in the following way: When

$$\frac{\delta_z}{2}\left(\frac{\tau}{\tau_c}\right)^2 \ll 1 \tag{26}$$

then

$$1 + \frac{\delta_z}{2}(\tau/\tau_c)^2 \simeq e^{(\delta_z/2)(\tau/\tau_c)^2} \tag{27}$$

so that expression 8 can be approximated as

$$|G^{(1)}(\tau)| = A^{1/2}e^{(-\tau/\tau_c)+[(\delta_z/2)(\tau/\tau_c)^2]} \tag{28}$$

If $(\delta_z/2)(\tau/\tau_c)^2 = 0.15$, for example, the difference between the two expressions is only 1%. When the logarithm of expression 28 is taken, a quadratic equation results:

$$\ln |G^{(1)}(\tau)| = d + b\tau + a\tau^2 \tag{29}$$

with

$$b = -1/\tau_c = -\langle D\rangle_z K^2 \tag{30}$$

and

$$\delta_z = 2a\tau_c^2 = 2a/b^2 \tag{31}$$

Knowing K, $\langle D\rangle_z$ and δ_z are readily determined from a and b. Since the photopulse autocorrelation function, $G^{(2)}(\tau)$, is related to $|G^{(1)}(\tau)|$ as $G^{(2)}(\tau) = A|G^{(1)}(\tau)|^2 + B$ (eq 11), a and b are determined by fitting the logarithm of the square root of the base line corrected ACS to expression 29. This procedure is more or less standard in using the method of cumulants to analyze PCS data.[6,9] The determination of the base line, B, is critical and deserves comment. For good samples with no anomalous scattering, the base line of the unclipped ACS can be computed knowing the correlator single channel counting rates.[4] The Langley–Ford correlator provides this information in several dedicated channels, and these are used to calculate B. To ensure the quality of the spectra generally and the validity of the base line calculation in particular, after a visual check of the sample, the spectra used in the work presented here were carefully monitored. In all cases, the scope trace of the ACS evolved smoothly and evenly, and no evidence of any anomalous scattering was observed either in the ACS or on the digital frequency meter used to monitor the scattered intensity directly. Furthermore, the correlator overflow monitor light never lit up. Finally, the computer printout which displays the contents of the correlator dedicated channel that accumulates any overflow counts in the course of a run always reads zero. Both the overflow light and the counter are known to function properly.

To fit the spectra of $\ln |G^{(1)}(\tau)|$ as described above, the 1% approximation was chosen, i.e.,

$$\tau_{max} = \tau_c(0.3/\delta_z)^{1/2} \tag{32}$$

This means that for a polydisperse system, the maximum correlator time delay, τ_{max}, considered in the analysis must be restricted. The more monodisperse the sample, the larger and less restrictive is τ_{max}. With a judicious choice of correlator sample time, it is usually possible to include enough points to guarantee a good fit to the data. Typically, spectral fits included about 50 points in this study.

In ref 6, it is claimed that the best estimate of δ_z is obtained by including successively fewer ACS points in fitting the spectrum and then extrapolating the corresponding δ_z estimates to zero delay time. This premise was easy to check since the polynomial fit routine used to obtain the fit coefficients a and b also provides the statistical (fit) uncertainties associated with them. Since $\delta_z = 2a/b^2$, the fit uncertanties associated with estimates of δ_z are easy to calculate. A number of spectra were fit using a maximum number of points that correspond to a spectral range extending from about $\tau_c/3$ to about $2\tau_c$. It was found that the minimum statistical error in δ_z generally occurs around $1\tau_c$. This result is consistent with earlier experience.[7] Fits using significantly fewer points had poor statistical quality and generally grossly overestimated δ_z and were definitely not suitable for use in analysis. As a consequence of this result, correlator sample times were chosen so as to provide roughly one characteristic relaxation time, $1\tau_c$, in the maximum number of channels (55) available for fitting. Again, there were typically about 50 channels used in each fit. Oftentimes, all 55 points were used. Occasionally, fewer points were used. When this occurred, it resulted solely from the application of the τ_{max} criterion, eq 32.

Discussion of Results

Preliminary PCS $\langle D\rangle_z$ and δ_z ($\delta_z \approx 0$) measurements of Pressure Chemical's 200 000 mol wt polystyrene standard, PC-1C, were in excellent agreement with earlier PCS $\langle D\rangle_z$ measurements of the same standard made by other investigators[10] in the course of their determination of the dependence of polystyrene's diffusion coefficient in 2-butanone on its molecular weight. For this reason, it was decided to use C and ν determined in this earlier work to investigate the range of validity of expressions 19 and 20 in measuring $\bar{M}_w$ and $\bar{M}_n$. Well-characterized polystyrene samples having molecular weights around 200 000 were chosen for this study both because of the PC-1C agreement and because they fall comfortably in the middle of the molecular weight range considered in ref 10. These values of $C = 5.5 \times 10^{-4}$ and $\nu = 0.561$ would presumably accurately relate extrapolated zero concentration values of $\langle D\rangle_z$ and molecular weight for the chosen standards. The results presented here bear out the validity of that presumption.

The concentration dependence of $\langle D\rangle_z$ and δ_z for the four polystyrene standards in 2-butanone at room temperature (21–22 °C) was measured. All measurements were made at a scattering angle of 90°. The four standards used

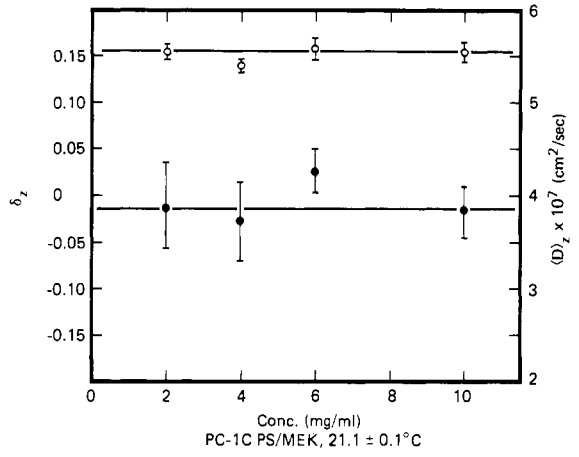

Figure 4. PCS concentration study results for PC-1C. δ_z and $\langle D \rangle_z$ are indicated by solid and open circles, respectively.

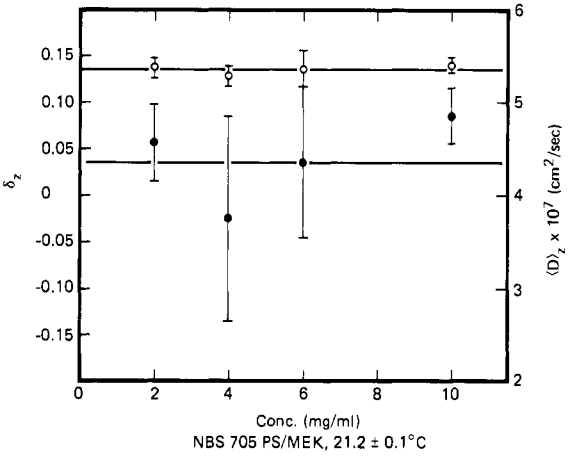

Figure 5. PCS concentration study results for NBS 705. δ_z and $\langle D \rangle_z$ are indicated by solid and open circles, respectively.

Table I

sample	$\langle D \rangle_z \times 10^7$, cm^2/s	δ_z
PC-1C	5.86 ± 0.06	−0.003 ± 0.026
NBS 705	5.66 ± 0.09	0.050 ± 0.025
PC-50124	4.89 ± 0.06	−0.003 ± 0.028
NBS 706	4.37 ± 0.03	0.101 ± 0.008
blend	5.22 ± 0.06	0.078 ± 0.023

were NBS 705, NBS 706, PC-1C, and PC-50124. The results of these concentration studies are presented in Figures 4 through 7. The error bars represent the standard deviation of a set of runs (typically 5) made at each concentration. The manufacturers and independently determined gel-permeation chromatographic (GPC) values for $\bar{M}_n$ and $\bar{M}_w$ for these standards are presented in Table II. From Figures 4 through 7, it is apparent that there was little or no diffusion coefficient concentration dependence in these samples. As a consequence, it is expected that the relative dispersion in $\langle D \rangle_z$ be independent of polymer concentration.[6] This expectation is consistent with the δ_z results in the figures.

To improve the statistical quality of the results for the molecular weight determinations, the four standards were each measured again—this time 20 runs apiece. Any run whose $\langle D \rangle_z$ value was 4σ or more away from the mean value of the set was eliminated from consideration. In addition, in each set of 20, a few runs were rejected because the results were scrambled in transmitting the data through to the 360/168. Consequently, about 15 runs are represented in each of the entries presented in Table I. A run typically took 1–2 min. The photodetection count rate varied between about 50 000 and 150 000 Hz while sample times of 1 or 2 μs were used. The quality factor, i.e., the ratio of the height of the zero-delay ACS point above the base line to the base line, varied from approximately 0.2 to approximately 0.4. It is worth mentioning that for all standards, the preliminary results, the concentration study results, and the "many-run" results were always in excellent agreement even though these measurements were made over several months during which time the sample cell was disassembled and reassembled and the alignment

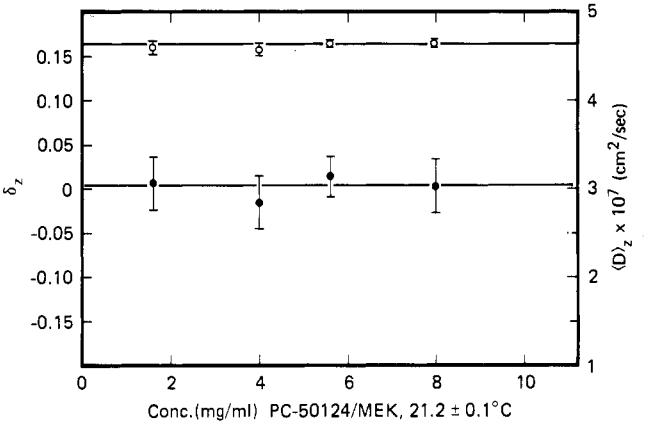

Figure 6. PCS concentration study results for PC-50124. δ_z and $\langle D \rangle_z$ are indicated by solid and open circles, respectively.

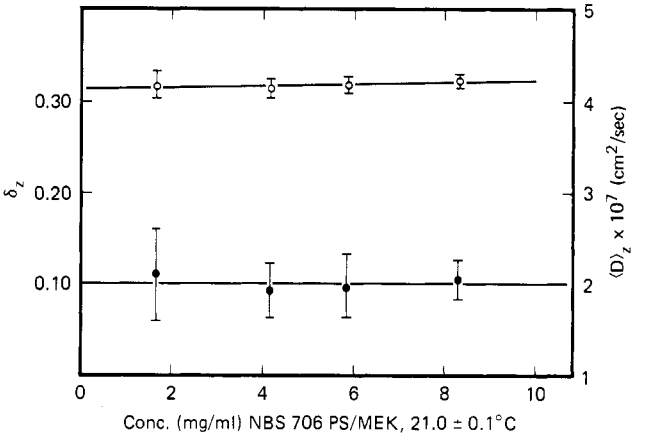

Figure 7. PCS concentration study results for NBS 706. δ_z and $\langle D \rangle_z$ are indicated by solid and open circles, respectively.

Table II

sample	PCS $\bar{M}_w$	PCS $\bar{M}_n$	PCS $\bar{M}_w/\bar{M}_n$	GPC $\bar{M}_w$	GPC $\bar{M}_n$	GPC $\bar{M}_w/\bar{M}_n$	manufacturer $\bar{M}_w$	manufacturer $\bar{M}_n$	manufacturer $\bar{M}_w/\bar{M}_n$
PC-1C	199 000	199 000	1.00	195 000	180 000	1.08	200 000	193 000	1.04
NBS 705	205 000	171 000	1.20	190 000	172 000	1.11	190 000 (SE), 179 000 (LS)	171 000	1.05-1.11
PC-50124	274 000	274 000	1.00	274 000	247 000	1.11	254 000	218 000	<1.06-1.17
NBS 706	317 000	179 000	1.77	262 000	144 000	1.82	288 000 (SE), 258 000 (LS)	137 000	1.88-2.10
blend	233 000	169 000	1.38	218 000	178 000	1.22			

checked and rechecked, etc. Note that the Table I $\langle D \rangle_z$ entries have been temperature and viscosity corrected to 25 °C so that they may be used with C and ν in the molecular weight calculations. To fill out the study, a blend of equal parts by weight of PC-1C, PC-50124, and NBS 705 was also measured. Based on the previous results, this blend was run 20 times at a single concentration of 0.42%. These $\langle D \rangle_z$ and δ_z results are presented in Table I, and the corresponding $\bar{M}_n$ and $\bar{M}_w$ results are presented, along with those of the four standards, in Table II.

From the results in Table II, it is seen that excepting NBS 706, there is good general agreement between PCS, GPC, and the manufacturers molecular weight determinations. Apparently, the molecular weight distribution of NBS 706 is too wide and too skewed and ν is not sufficiently close to 1 for its $\bar{M}_n$ and $\bar{M}_w$ values to be accurately measured using the PCS methods developed in this paper. Although the NBS 706 δ_z value is a little too large to fit onto the $\nu = 0.561$ curve of Figure 1, the value of $\bar{M}_w/\bar{M}_n$ estimated from this curve, 1.77, is in good agreement with the manufacturer's and the GPC values. $\bar{M}_w$ and $\bar{M}_n$ themselves, however, are somewhat too high. The origin of this discrepancy lies in the magnitudes of the skewness and higher moments of the 706 molecular weight distribution. From the GPC $\bar{M}_z/\bar{M}_w$ value (not presented in the table) and δ_{2n}, δ_{3n} can be calculated following a procedure analogous to that used to relate $\bar{M}_w/\bar{M}_n$ to δ_{2n}. The result is:

$$\bar{M}_z/\bar{M}_w = \frac{\langle M \rangle_n \langle M^3 \rangle_n}{\langle M^2 \rangle_n^2} = \frac{1 + 3\delta_{2n} + \delta_{3n}}{(1 + \delta_{2n})^2} \quad (33)$$

or

$$\delta_{3n} = \left(\frac{\bar{M}_w}{\bar{M}_n}\right)^2 \frac{\bar{M}_z}{\bar{M}_w} - 3\frac{\bar{M}_w}{\bar{M}_n} + 2 \quad (34)$$

In its own right, expression 33 is interesting because it reveals the nature of the dependence of $\bar{M}_z/\bar{M}_w$ on the breadth of the molecular weight distribution. Even when the skewness of the distribution is zero, $\bar{M}_z/\bar{M}_w$ is >1 since δ_{2n} is not zero. Using the GPC values $\bar{M}_z/\bar{M}_w = 1.82$ and $\bar{M}_z/\bar{M}_w = 1.52$, δ_{3n} is calculated to be 1.57. Substituting these δ_{2n} and δ_{3n} values into expression 18, a value of $\delta_z = 0.25$ is computed. Since the measured value of δ_z is 0.10, apparently the fourth and higher moments in the molecular weight distribution of NBS 706 combine to reduce the influence of the skewness leaving a value of δ_z which coincidentally yields a reasonable estimate of δ_{2n} and thus $\bar{M}_w/\bar{M}_n$. The influence of the fourth and higher moments is also seen by calculating $\langle D \rangle_z$ using δ_{2n} and δ_{3n} in eq 15. The calculated $\langle D \rangle_z$ is 3.23×10^{-7} cm^2/s, whereas the measured value (at 25 °C) is 4.40×10^{-7} cm^2/s. Again, moments higher than the third, which have not been accounted for in eq 15, give rise to a discrepancy between the measured and computed values of $\langle D \rangle_z$. From these results, it is clear that the molecular weight distribution of NBS 706 is not only broad and skewed but has non-negligible higher moments as well. These results are consistent with two careful GPC analyses of NBS 706 which found it to be somewhat bimodal with a distinct lower molecular weight "bump" in addition to the main peak.[11]

The results for PC-1C and PC-50124 are in good agreement with the GPC and Manufacturer's $\bar{M}_w$ and $\bar{M}_n$ results, but in both cases, PCS found these standards to be "effectively" monodisperse, $\delta_z \approx 0$. Apparently, when $\bar{M}_w/\bar{M}_n \lesssim 0.05$–$0.10$, PCS results analyzed by the method of cumulants yield $\delta_z \approx 0$. This limitation stems, at least in part, from a reduction in the impact of the polydispersity, δ_{2n}, on δ_z through multiplication of δ_{2n} by the factor ν^2. This reduction in the effect of polydispersity is useful, though, because it allows samples of greater polydispersity to be measured.

Next the results for NBS 705 are considered. These results are interesting because while NBS 705 and PC-1C are both supposed to be essentially monodisperse samples very close in molecular weight, repeated measurements at different times on these two samples, while self-consistent, were consistently different—as seen in Tables I and II. The PCS result shows NBS 705 to be a broader distribution than that found either by NBS or by independent GPC determination. This "extra" polydispersity in NBS 705 has been noted before and results from an unobtrusive higher molecular weight shoulder in the NBS 705 molecular weight distribution.[12] Apparently, PCS is sensitive to the presence of this shoulder while fractionation and routine GPC alone are not. In this regard, it is interesting to note that spectral inversion of PCS measurements of NBS 705 was apparently insensitive to the presence of this shoulder.[5] The GPC and PCS results for the polystyrene standard blend are in reasonably good agreement. The fact that PCS measures a greater polydispersity in this sample originates presumably from the higher molecular weight shoulder in the NBS 705 that was "hidden" from the GPC.

Finally, it is worth mentioning that the methods developed here can be used to determine the power-law constants, C and ν, from one series of runs on a single sample. This could be done as follows: Accurately measure $\bar{M}_w$ and $\bar{M}_n$ for a representative sample of the polymer of interest. Arrange it so that $\bar{M}_w/\bar{M}_n$ is about 1.5, a value that could readily be achieved by fractionation, for example. Measure $\langle D \rangle_z$ and δ_z over a suitable concentration range, and determine their infinite dilution values. From eq 19 and 20, C and ν can then be calculated. This procedure requires considerably less effort than running $\langle D \rangle_z$ concentration studies on a series of (hopefully) very narrow distribution samples. The power-law constants obtained should be valid at least in the molecular weight decade of the measured sample.

Comment

It is very important to have accurate values of C and ν in employing the method of determining $\bar{M}_w$ and $\bar{M}_n$ developed in this paper. The values used in this work, those of ref 10, gave generally good estimates of $\bar{M}_n$ and $\bar{M}_w$ when compared with the manufacturer's and GPC results. At least one other inelastic light-scattering study of the relationship between the infinite dilution diffusion coefficient of polystyrene in 2-butanone at 25 °C and its molecular weight exists.[13] This second study covers the same molecular weight range as ref 10. Both sets of C and ν were tried on the $\langle D \rangle_z$ and δ_z values measured in this study, and while those of ref 10 yielded good results, those of ref 12 gave $\bar{M}_w$ and $\bar{M}_n$ values consistently below those reported by the manufacturers and those determined by GPC. Despite the conclusions of yet another inelastic light-scattering study[14] which finds the C and ν results of ref 13 preferable to those of ref 10, the extensive results presented here support the validity of the C and ν values reported in (10).

Conclusions

Subject to certain restrictions, the method of cumulants can be used to analyze the autocorrelation spectra of light scattered inelastically from dilute polymer solutions in order to obtain the polymer number-averaged and weight-averaged molecular weights. By reversing the molecular weight determination procedure, a single,

well-characterized, and representative polymer sample can be used to calculate the power-law constants, C and ν, in the relationship $D = CM^{-\nu}$, where D is the infinite dilution z-averaged diffusion coefficient of the polymer sample.

Acknowledgment. It is a pleasure to thank A. C. Ouano and R. Pecora for taking their time to discuss the contents of this paper, L. Rosen of Pressure Chemical Co. for suggesting the blending of polymer standards of comparable molecular weights, and M. Berkenblit and T. Horikawa for technical assistance.

References and Notes

(1) J. R. Urwin in "Light Scattering from Polymer Solutions", M. B. Huglin, Ed., Academic Press, New York, 1972.
(2) H. Hack and G. Meyerhoff, *Makromol. Chem.*, **179**, 2475 (1978).
(3) B. J. Berne and R. Pecora, "Dynamic Light Scattering–With Applications to Chemistry, Biology and Physics", Wiley, New York, 1976, Chapter 8.
(4) D. E. Koppel, *J. Chem. Phys.*, **57**, 4814 (1972).
(5) S. W. Provencher, J. Hendrix, and L. DeMaeyer, *J. Chem. Phys.*, **69**, 4273 (1978); E. Gulari, E. Gulari, Y. Tsunashima, and B. Chu, *Polymer*, **20**, 347 (1979).
(6) J. C. Brown, P. N. Pusey, and R. Dietz, *J. Chem. Phys.*, **62**, 1136 (1975).
(7) J. C. Selser, Y. Yeh, and R. J. Baskin, *Biophys. J.*, **16**, 337 (1976).
(8) J. C. Selser and Y. Yeh, *Biophys. J.*, **16**, 847 (1976).
(9) P. N. Pusey in "Photon Correlation and Light Beating Spectroscopy", H. Z. Cummins and E. R. Pike, Eds., Plenum Press, New York, 1974.
(10) T. A. King, A. Knox, and J. D. G. McAdam, *Polymer*, **14**, 293 (1973).
(11) A. C. Ouano, private conversation. L. J. Fetters, private conversation.
(12) A. C. Ouano, *J. Colloid Interface Sci.*, **63**, 275 (1978); L. J. Fetters, *J. Appl. Polym. Sci.*, **20**, 3437 (1976); D. Plazek and P. Agarwal, *ibid.*, **22**, 2127 (1978).
(13) N. C. Ford, F. E. Karasz, and J. E. M. Owen, *Discuss. Faraday Soc.*, **49**, 228 (1970).
(14) M. E. McDonnell and A. M. Jamieson, *J. Macromol. Sci. Phys.*, **13**, 67 (1977).

Polymer Molecular Weight Determination Using Liquid Crystals

Bengt Kronberg[1] and Donald Patterson*

Otto Maass Chemistry Building, McGill University, 801 Sherbrooke Street West, Montreal, Quebec H3A 2K6, Canada. *Received March 1, 1979*

ABSTRACT: The thermodynamic treatment of the freezing-point depression is applied to the solute-induced depression of the nematic–isotropic transition temperature for a liquid-crystal solvent. It is shown that it should be possible to determine solute molecular weights up to $\sim 10^6$. The method is applied to samples of two polymers, polystyrenes and poly(ethylene oxides), dissolved in two different liquid crystals, *N*-(*p*-ethoxybenzylidene)-*p*-*n*-butylaniline (EBBA) and *p*-azoxyanisole (PAA). Molecular weights up to 10^5 are determined with an accuracy of $\sim 20\%$.

It has recently been shown[2] that the two polymers, polystyrene and poly(ethylene oxide), are soluble in the nematic and isotropic phases of the liquid crystal *N*-(*p*-ethoxybenzylidene)-*p*-*n*-butylaniline (EBBA). We show here that an accurate molecular weight determination of the polymer in a thermotropic liquid-crystal solvent is possible, using the polymer-induced depression of the nematic–isotropic transition temperature. At least in principle, the determination should remain accurate to molecular weights of $\sim 10^6$, whereas the usual cryoscopic technique cannot be used beyond $\sim 3 \times 10^4$.

In a nematic liquid crystal, the rodlike molecules are aligned with their long axes parallel. At the nematic–isotropic transition, this long-range order is completely destroyed. This is a first-order transition, and it can therefore be subjected to a thermodynamic treatment analogous to that of the melting of a crystal. The effect of a polymeric solute in the nematic phase of a liquid-crystal solvent is a decrease of the nematic order, and hence the nematic–isotropic transition temperature will be lowered. The transition is not sharp, as in the pure liquid crystal, but occurs over a temperature range where the nematic and isotropic phases are in equilibrium. This is illustrated in the schematic phase diagram in Figure 1. Here the lower $(T,w_2)^N$ boundary indicates were the isotropic phase first appears on heating, while the upper $(T,w_2)^I$ boundary indicates where the nematic phase first appears on cooling. The two-phase boundaries meet at the single nematic–isotropic transition temperature of the pure solvent, T_1^0. The shape of the two-phase boundaries has been discussed elsewhere.[2,3]

Cryoscopic and Liquid-Crystal Determinations of Molecular Weights. The cryoscopic determination of solute molecular weight is based on the freezing-point depression as given by the familiar van't Hoff equation:[4]

$$\Delta T = \frac{R(T_1^0)^2}{1000\Delta h_1^0} m_2 = Km_2 \tag{1}$$

Here K is the molal freezing-point constant (in units of deg mol^{-1}) and m_2 is the molal concentration of the solute. The pure solvent freezes at T_1^0 with a latent heat of fusion, Δh_1^0, expressed per gram. Rearranging the equation to yield the unknown molecular weight gives

$$M_2 = \frac{R(T_1^0)^2}{\Delta h_1^0} \frac{w_2}{\Delta T} \tag{2}$$

where w_2 is the weight fraction of the solute in the liquid solution.

Rothmund[5] has extended the van't Hoff freezing-point equation to include the case where the solute forms a mixed crystal with the solvent. The solute molecular weight is now obtained through

$$M_2 = \frac{R(T_1^0)^2}{\Delta h_1^0 \Delta T}(w_2^{\text{liquid}} - w_2^{\text{crystal}}) \tag{3}$$

which reverts to the van't Hoff equation if $w_2^{\text{crystal}} = 0$.

A detailed thermodynamic treatment of liquid-crystal + solute-phase diagrams has previously been given,[2,3] and the results show that there is a complete analogy between the depression of the nematic–isotropic transition tem-

0024-9297/79/2212-0916$01.00/0